

Application of hand-held near-infrared and Raman spectrometers in surface treatment authentication of cork stoppers

Jorge Mellado-Carretero^a, Didem Peren Aykas^{b,c}, Miquel Puxeu^d, Sylvana Varela^e,
Luis Rodriguez-Saona^b, Diego García-Gonzalo^f, Sílvia de Lamo-Castellví^{a,*}

^a Departament d'Enginyeria Química, Universitat Rovira i Virgili, Av. Països Catalans 26, Campus Sescelades, 43007, Tarragona, Spain

^b Department of Food Science and Technology, Ohio State University, 2015 Fyffe Rd, Columbus, Ohio, 43210, USA

^c Department of Food Engineering, Faculty of Engineering, Adnan Menderes University, Aydın, 09100, Turkey

^d Àrea de Química enològica, Parc Tecnològic del Vi (VITEC), Carretera de Porrera, Km. 1, 43730, Falset, Spain

^e Departament d'Enginyeria Mecànica, Universitat Rovira i Virgili, Av. Països Catalans 26, Campus Sescelades, 43007, Tarragona, Spain

^f Tecnología de los Alimentos, Instituto Agroalimentario de Aragón-IA2 (CITA-Universidad de Zaragoza), Miguel Servet 177, 50013, Zaragoza, Spain

ARTICLE INFO

Keywords:

Hand-held

Cork

Multivariate analysis

Spectroscopy

Surface treatment

ABSTRACT

The aim of this paper was to evaluate the potential of using near-infrared (NIR) spectroscopy and multivariate analysis as a rapid tool to non-destructively determine the presence of surface treatments applied to cork stoppers. Density and dimensions of 6 closure varieties were characterized and the extraction force was measured on those produced for still wines. Cork stoppers were also analyzed using hand-held NIR and Raman spectrometers. Soft independent modelling of class analogy (SIMCA) models showed significant differences among treated and untreated samples, linked to components of the coating agents applied (silicone and paraffin). SIMCA model's classification performance was tested and high sensitivity (93.33 %) and specificity (100 %) values were obtained. Partial least squares regression (PLSR) model accurately predicted the extraction forces measured with low standard error of prediction (SEP = 4.0 daN). Our results are promising for the future application of this technology in cork industry, reducing time and economic losses.

1. Introduction

Cork, a natural material obtained from the bark of the cork oak (*Quercus suber* L.), has been used for stopping wine containers during more than 2000 years. Different physicochemical properties make cork suitable for its use as a wine closure, such as compressibility, resilience, high friction coefficient, imperviousness to liquids, chemical inertness and air permeability (Jackson, 2014; Pereira, 2007b; Silva et al., 2008). Consequently, cork stoppers prevent any leakage, do not negatively change chemical and sensorial characteristics of wine and allow an adequate oxygen transfer (Pereira, 2007b).

Because of the strong friction forces between cork and glass, cork stoppers have to be treated with several food grade coating agents, being paraffin and silicone the most commonly used. Moreover, such agents restore the imperviousness lost during the processing steps of cork manufacturing and improve their sealant properties by filling imperfections in the cork surface. The hydrophobic properties of paraffin help to reduce wine leaks and prevent the migration of potential taints from

the stopper to the wine. However, this treatment can aggravate the stopper extraction when it is applied without slipping additives. Therefore, paraffin is usually covered up with a layer of silicone (polydimethylsiloxane) in order to lubricate the stopper and simplify its insertion and extraction from the bottle (Fugelsang, Callaway, Toland, & Muller, 1997; Pereira, 2007a; Silva et al., 2008). Accordingly, it is imperative to check the presence of surface treatments applied to cork stoppers, otherwise the uncorking of those bottles sealed with nonproper treated stoppers becomes impossible, leading to their disposal.

At present, different methods have been proposed for the analysis of surface treatments applied to cork stoppers. The presence of surface treatments is indirectly assessed by measuring the extraction or torque forces for still wine stoppers and sparkling wine stoppers, respectively. Additionally, a simple test can be applied by examining the capillarity effect on the surface of cork stoppers by standing them upright in a colored liquid (Jung & Schaefer, 2010). Even though both tests are a simple way to check the presence of surface treatments, they cannot distinguish the different components applied on the cork and do not

* Corresponding author.

E-mail address: silvia.delamo@urv.cat (S. de Lamo-Castellví).

<https://doi.org/10.1016/j.fpsl.2021.100680>

Received 10 July 2020; Received in revised form 29 April 2021; Accepted 2 May 2021

Available online 8 May 2021

2214-2894/© 2021 The Author(s).

Published by Elsevier Ltd.

This is an open access article under the CC BY-NC-ND license

(<http://creativecommons.org/licenses/by-nc-nd/4.0/>).

provide information about the homogeneity of their distribution (González-Adrados et al., 2012).

Infrared spectroscopy has been used for cork quality assessments since it rapidly provides a chemical fingerprint of the different components that lie in its heterogeneous matrix (Fernández Pierna, Manley, Dardenne, Downey, & Baeten, 2018). Ortega-Fernández, González-Adrados, García-Vallejo, Calvo-Haro, and Cáceres-Esteban (2006) could successfully determine the dose and type of several surface treatments applied to cork stoppers by using attenuated total reflectance Fourier transform mid-infrared (ATR-FT-MIR) spectroscopy combined with powerful pattern recognition techniques. Moreover, González-Gaitano and Ferrer (2013) provided several parameters obtained from ATR-FT-MIR spectra for the quantification of surface treatments applied in several cork stoppers. Nonetheless, FT-MIR spectroscopy cannot be applied for on-line process monitoring since it implies the preparation and destruction of the samples, leading to time and economic losses for the manufacturers.

Near-infrared (NIR) spectroscopy has been used to quantitatively determine different physicochemical and mechanical parameters of cork (i.e. moisture, porosity, visual quality, etc.) and to classify cork stoppers by variety and origin (Prades, García-Olmo, Romero-Prieto, García de Ceca, & López-Luque, 2010; Prades, Gómez-Sánchez, García-Olmo, González-Hernández, & González-Adrados, 2014; Sánchez-González, García-Olmo, & Prades, 2016). Its low instrumentation costs (when compared to MIR technology) and the possibility to implement it on-line in a non-destructive way makes NIR spectroscopy a suitable technique for the assurance of the surface treatments applied on cork stoppers (McClure et al., 2006; Porep, Kammerer, & Carle, 2015).

For this reason, the present work aims to validate NIR spectroscopy combined with multivariate analysis as a rapid and powerful tool used to non-destructively determine the presence of surface treatments applied to cork stoppers. Physical parameters to evaluate the surface treatments administered such as extraction force were also studied and compared with the technology proposed herein. Additionally, the feasibility of Raman spectroscopy for the surface treatment monitoring of cork stoppers was also tested. The results provided in this paper are promising for the future application of NIR spectroscopy for quality control assessments in the cork industry.

2. Materials and methods

2.1. Cork stopper samples

Six cork closure varieties were provided by a regional cork stopper

manufacturer (Fig. S1); including natural cork stoppers for still wines (N-S), technical cork stoppers consisting of agglomerated cork (particle size of 2–7 mm) with two end discs of natural cork for still and sparkling wines (AD-S and AD-SP, respectively), micro-agglomerated cork stoppers (particle size of 0.5–2 mm) for still wines and sparkling wines (M-S and M-S P, respectively) and cork stoppers made of a mixture of agglomerated and micro-agglomerated cork for sparkling wines (A/ M-S P). The composition of all body-agglomerated cork stoppers was 75 % cork granules and 25 % binder (polyurethane; information provided by the supplier).

Each variety consisted of 48 closures, 24 of them treated and the rest untreated in order to take them as a reference. Silicone (polydimethylsiloxane) treatments were applied with a pneumatic gun at room temperature, which projected the lubricating product on the moving corks in an industrial revolving stainless-steel drum (20 rpm for 1–2 min). The stoppers were subsequently left for 30 min more inside the drum. For N-S cork stoppers, paraffin was added prior to silicone and placed into the drum in a solid form (20 rpm at 35–40 °C for 30 min). Samples analyzed in this study and the type of treatment applied to them are summarized in Table 1.

2.2. Physical assays

The mean diameter, ovalization, height, mass and apparent density of cork stoppers were measured according to the Spanish UNE standards (Asociación Española de Normalización y Certificación, 2001, 2003, 2006, 2019). Before performing the physical and mechanical assays, cork stoppers were conditioned for 24 h at 20 °C and 65 % relative humidity. Diameters and heights were measured using a caliper with 0.01 mm precision. The mean diameter (D ; expressed in mm) was obtained by the average of the diameters measured at parallel (D_1 ; in mm) and perpendicular directions (D_2 ; in mm) to the growth lines of the cork (Eq. 1):

$$D = \frac{D_1 + D_2}{2} \quad (1)$$

The apparent density (d ; in kg/m^3) was then obtained from the Eq. 2 (natural and agglomerated still wine cork stoppers):

$$d = \frac{4 \times 10^6 \times m}{\pi \times D^2 \times h} \quad (2)$$

where m is the mass in g, D is the mean diameter expressed in mm, and h is the height in mm. For natural cork stoppers, the ovalization (OV; in mm) was calculated by subtracting diameters D_1 and D_2 (in mm) and

Table 1
Physical properties of cork stoppers analyzed in this study.

Cork stopper	Treatment applied	Dose (mg/stopper)	Diameter (mm)	Height (mm)	Ovalization (mm)	Mass (g)	Density (kg/m^3)
N-S	Untreated		24.0 ± 0.1^a	44.4 ± 0.1	0.1 ± 0.1	NA	177 ± 26
	Paraffin and silicone	9 (paraffin) 12 (silicone)	24.0 ± 0.1	44.1 ± 0.2	0.1 ± 0.1	NA	174 ± 17
AD-S	Untreated		23.3 ± 0.1	43.9 ± 0.1	NA	NA	272 ± 9
	Silicone ^b	12	23.4 ± 0.1	44.0 ± 0.1	NA	NA	276 ± 10
M-S	Untreated		23.9 ± 0.1	42.2 ± 0.2	NA	NA	283 ± 5
	Silicone	12	24.8 ± 0.1	43.8 ± 0.8	NA	NA	293 ± 10
AD-SP	Untreated		30.3 ± 0.1	48.1 ± 0.2	NA	9.2 ± 0.3	NA
	Silicone	37	30.8 ± 0.1	48.1 ± 0.1	NA	9.2 ± 0.2	NA
A/ M-S P	Untreated		30.3 ± 0.1	48.0 ± 0.1	NA	9.6 ± 0.2	NA
	Silicone	37	29.8 ± 0.1	48.0 ± 0.1	NA	9.3 ± 0.2	NA
M-S P	Untreated		30.9 ± 0.0	48.2 ± 0.1	NA	9.6 ± 0.2	NA
	Silicone	37	30.3 ± 0.1	48.0 ± 0.1	NA	9.5 ± 0.2	NA

Abbreviations used: N-S, natural cork-still wine; AD-S, agglomerated cork with discs-still wine; M-S, micro-agglomerated cork-still wine; AD-SP, agglomerated cork with discs-sparkling wine; A/ M-S P, Mixture agglomerated/micro-agglomerated cork-sparkling wine; M-S P, micro-agglomerated cork-sparkling wine. NA, not applicable according to UNE standards.

^a Values are means of twenty-four replicates \pm standard deviation (SD).

^b Silicone oil.

expressed in absolute value (Eq. 3):

$$OV = |D_1 - D_2| \quad (3)$$

2.3. Mechanical assays: extraction force

The extraction force was measured following UNE standards with minor modifications (Asociación Española de Normalización y Certificación, 2001, 2003, 2006, 2019). First, corking was accomplished using a semi-automatic capping unit Officine Pesce model PG91 RN (Officine Pesce Snc, Bubbio, Italy). The bottles (Bordeaux type, with 18.5 mm bottleneck) were previously filled with a hydroalcoholic solution (12 % ethanol with 5 g/L of tartaric acid adjusted to pH = 3.5 with sodium hydroxide), and then left in an upright position. After 24 h, the cork stoppers were removed using an ExtraLab Portable (EGITRON, Mozelos, Portugal) and the maximum value of the extraction force was subsequently recorded in daN. Twelve cork stoppers of each variety were analyzed in this study.

2.4. Diffusive reflectance near-infrared (NIR) spectroscopy

NIR spectra were obtained from different spots of each cork stopper (see Fig. S2; the spectra were taken considering the different sections of the cork plank from which the stopper came, since these could show differences on their physical properties) using a hand-held NIR analyzer Polychromix microPHAZIR (Thermo Scientific, Tewksbury, Massachusetts) with a scanning window of 4 mm (sampling area of 13 mm²) and equipped with a single InGaAs detector. NIR spectra were collected in the region of 1600–2400 nm with 8 nm resolution from the average of 64 scans to improve the signal-to-noise ratio. A background spectrum was collected with a highly reflective gold-coated reference material before every measurement to prevent the environment's contribution. Four independent stoppers were randomly selected and analyzed following the scheme depicted in Fig. S2, except for untreated N-S stoppers, in which twelve of them were analyzed for reproducibility testing purposes. The number of spectra (Table S1) in treated samples could vary (7–10 spectra taken) due to the presence of brand names printed with fire (Fig. S1).

2.5. Transmission Raman spectroscopy

Raman spectra were obtained using a hand-held Raman Progeny analyzer (Rigaku Raman Technologies Inc., The Woodlands, Texas) interfaced with a 1064 nm (excitation wavelength) laser and an InGaAs detector (sampling area of 500 μm²). Raman spectra were collected from 200–2500 cm⁻¹ (8–11 cm⁻¹ resolution) with a power of 150 mW and 1500 ms integration time. Only M-S P stoppers were analyzed in the present work.

2.6. NIR and Raman spectra preprocessing

NIR data pre-processing was performed using Pirouette 4.5 (Infometrix Inc., Washington, US). After mean centering, NIR data was corrected using a Multiplicative Scatter Correction (MSC; the mean of the entire data set was taken as the reference spectrum) algorithm and transformed to its second derivative through a second polynomial Savitzky-Golay filter of 7 points width.

Raman pre-processing was first accomplished using MATLAB 9.5 (The Mathworks Inc., Natick, Massachusetts, US). Spectra denoising was achieved using sym4 wavelets with two-level decomposition and soft minimax thresholding technique. Denoised spectra were then uploaded to Pirouette 4.5 to perform mean centering and MSC algorithms (the mean of each sample's data set was taken separately as the reference spectrum).

2.7. Multivariate analysis applied to Raman and NIR data

Soft independent modelling of class analogy (SIMCA) models were built up to study the capability of NIR and Raman data to discriminate and differentiate the treated corks from those without treatment. Models were interpreted in terms of class projections plots (i.e. PCA scores' plots), interclass distances and discriminating power (Wold & Sjöström, 1977; Wold, 1976). Outlier determination was performed according to sample residuals and Mahalanobis distances (Shah & Gemperline, 1990). SIMCA model's classification performance was tested using an external validation set consisting of one stopper per variety analyzed (5 treated closures (60 spectra in total) and 5 untreated (44 spectra); natural cork stoppers were not included in this set) and evaluated based on its sensitivity and specificity. The sensitivity is known as the percentage of samples coming from a certain class that are correctly identified by the model of that class, while specificity accounts for the percentage of samples belonging to other classes that are correctly rejected by that model (Bevilacqua et al., 2013). All the mentioned outputs were based on the individual spectra.

Calibration models were constructed based on the partial least squares regression (PLSR) method in order to correlate the reference values of extraction force with the NIR data. The number of latent variables selected was determined through an F test (probability level of 95 %) to assess which model had the lowest and statistically different prediction residual error sum of squares (PRESS) value (Osten, 1988). Models were interpreted in terms of regression vector and evaluated according to the coefficients of determination in calibration (R²_{CAL}) and validation (R²_{VAL}) and the standard error of cross-validation (SECV). In this regard, the cross-validation step was conducted using the leave-one-out approach. Studentized residuals and leverage values were used for outliers' assessment (Weisberg, 2005). PLSR model's performance was tested using an external validation set consisting of one stopper per variety analyzed and examined in terms of standard error of prediction (SEP).

2.8. Extraction force data analysis

A Welch's ANOVA test was conducted since the homoscedasticity assumption was not met (distributions' homoscedasticity and normality were tested through the Levene's test and Shapiro-Wilk's test, respectively). A Dunnett's T3 post-hoc test was performed to obtain pairwise comparisons among sample means in extraction force data. The significance level was set at $P < 0.05$ in all tests. These statistical analyses were conducted using the software IBM SPSS Statistics for Windows, version 25.0 (IBM Corp., New York, US).

3. Results and discussion

3.1. Cork stoppers' physical and mechanical characterizations

The UNE 56921 standard specifications for natural cork stoppers establishes ovalization values lower than 0.5 mm and apparent densities of 125–230 kg/m³ (Asociación Española de Normalización y Certificación, 2003). Both ovalization and apparent density values obtained for N-S stoppers were within the aforementioned ranges (Table 1). Concerning micro-agglomerated cork stoppers for still wines, the UNE 56933 standard states an acceptance range of apparent densities from 240 kg/m³ to 350 kg/m³ (Asociación Española de Normalización y Certificación, 2019), which is in agreement with the data obtained for M-S cork stoppers. AD-S cork stoppers also met the specifications of the UNE 56926 standard for apparent density values (235–315 kg/m³, Table 1) (Asociación Española de Normalización y Certificación, 2001). Furthermore, the mass of cork stoppers made for sparkling wines was measured as an indirect estimator of the density. The mean values of masses for AD-SP, A/ M-S P and M-S P were within the range stated by the UNE 56923 standard (8.4–10 g, Table 1) (Asociación Española de

Normalización y Certificación, 2006).

The extraction force measurements for the cork stoppers analyzed are shown in Fig. 1. The mean values for the extraction force in N-S, AD-S and M-S samples were consistent with the data from literature (mean values of 19.6 daN and 34.7 daN for natural and technical cork stoppers, respectively) (Giunchi, Versari, Parpinello, & Galassi, 2008), as well as they met the UNE standard specifications (20–40 daN for N-S and AD-S samples and 15–40 daN for M-S samples) (Asociación Española de Normalización y Certificación, 2001, 2003). Significant differences were observed in extraction force values between treated and untreated corks in N-S and AD-S samples, confirming through this indirect method the presence of surface-coating agents in N-S and AD-S cork stoppers. However, no significant differences were detected between treated and untreated M-S samples. Sánchez-González and Pérez-Terrazas (2018) stated that both, cork percentage and density provide a good indicator of the mechanical behavior of agglomerated cork stoppers. In their work, when comparing micro-agglomerated stoppers with the same cork percentage, those having higher densities displayed higher extraction force values. The fact that the treated and untreated M-S samples (same cork percentage) displayed differences in density (also dimensions, Table 1) could be a reason why the extraction force values recorded were similar.

3.2. Interpretation of raw NIR and Raman spectra

Raw NIR and Raman (denoised) spectra of treated and untreated cork stoppers are shown in Fig. 2. Since all NIR spectra looked very similar, only one obtained for one type of cork stopper is presented. The NIR spectra of cork stoppers (Fig. 2a) displayed the same profile as the ones reported previously (Prades, Gómez-Sánchez, García-Olmo, & González-Adrados, 2012, 2014). Several NIR bands were identified and related to the main components of the cork. The NIR band at 1725 nm corresponds to the CH vibrations (first overtone stretching) of lignin or hemicellulose, as well as the NIR bands at around 2300 and 2345 nm could be assigned to CH (C–H stretching + C–H deformation) and CH₂ (C–H bending + C–H stretching) groups of cellulose or hemicellulose. Additionally, other NIR bands were observed at 1927 and 2145 nm, the former being attributed to OH groups of water (O–H stretching + O–H deformation) and the latter to the CH and CO combination band (C–H stretching + C=O stretching) (2014, Prades et al., 2012; Schwanninger, Rodrigues, & Fackler, 2011; Workman & Weyer, 2008).

Regarding Raman spectra, the main Raman bands observed (Fig. 2b) were in accordance with previous results obtained for other wood species. The Raman bands located at 1603 and 1630 cm⁻¹ could belong to the aryl ring stretching vibrations of lignin and the ring conjugated C=C stretching vibrations of coniferaldehydes, respectively (Gierlinger & Schwanninger, 2006; Tshabalala, Jakes, VanLandingham, Wang, &

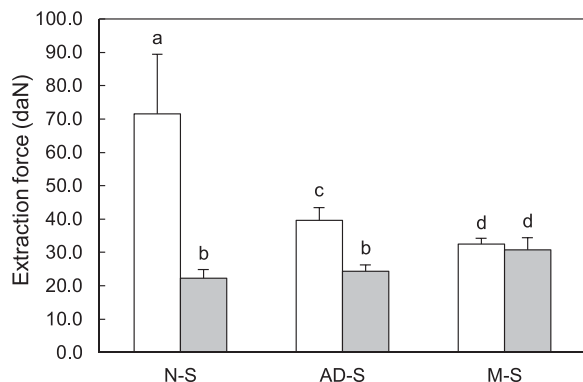


Fig. 1. Extraction force measurements for untreated (blank) and treated (grey) still wine stoppers inserted in an 18.5 mm diameter Burgundy type bottle, with and without surface treatment. Error bars in the plot represent the standard deviation for 12 independent replicates. Means with different letters are significantly different ($P < 0.05$).

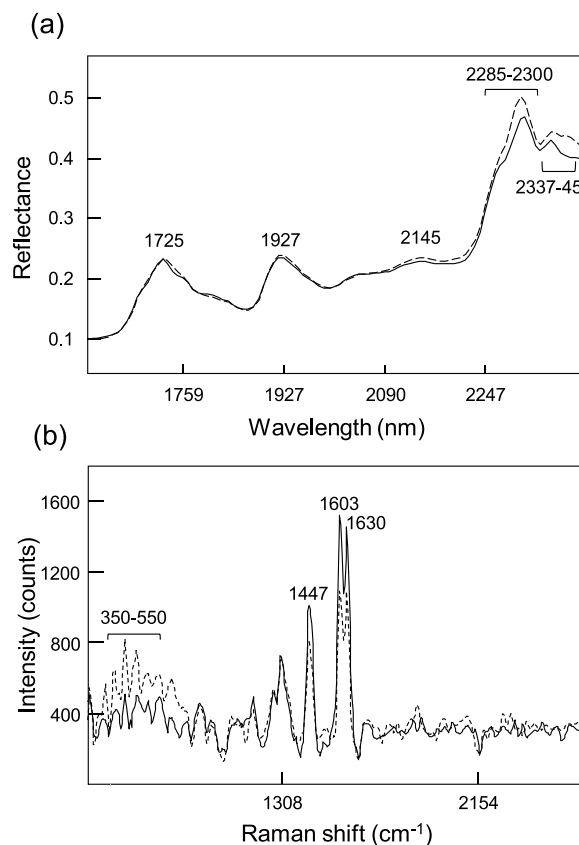


Fig. 2. (a) Near-infrared and (b) Raman spectra profiles of untreated (solid line) and treated (dashed line) cork stoppers (M-SP samples).

Peltonen, 2012). Moreover, the band at 1447 nm might be linked to guaiacyl ring vibrations of lignin. Several Raman bands were also displayed in the region of 350–550 cm⁻¹, and could be associated to the skeletal deformation of aromatic rings, substituent groups and side chains of lignin (Tshabalala et al., 2012).

3.3. Surface treatment authentication by NIR spectroscopy combined with SIMCA

A PCA-based pattern recognition method, SIMCA, was performed to obtain classification models in order to discriminate treated and untreated cork stoppers and to evaluate the chemical components that could make them different. Class projections plots (i.e., PCA scores' plots of the entire data set) of 2-class SIMCA models built up for NIR data (Fig. 3 and Table S1), each of them comprising treated and untreated corks for every type of stopper, were generated to visualize spectra reproducibility and class separation. The ellipses depicted in the plots represent the regions in which samples from a certain class fall into with a 95 % of confidence (Kvalheim & Karstang, 1992). Every data point in the figure (a 2D representation of a 3D graph) represents one sample's spectrum. All the classes were tightly clustered and well separated (not overlapped, Fig. 3), indicating discrimination among treated and untreated cork stoppers regardless of their variety. However, some of the outliers detected (Table S1), which belonged to treated cork stoppers spectra, were classified as untreated samples. These results suggest that the surface treatments applied were not entirely homogeneous.

An alternative approach to study class separation is the interclass distance (ICD) value. In SIMCA, PCA models for every class in the training set are performed, and then the residuals are computed by fitting the objects of every training set's class to the PCA model of each class. The overall standard deviations of that residuals are used to calculate the ICD value, which is a ratio of interclass to intraclass

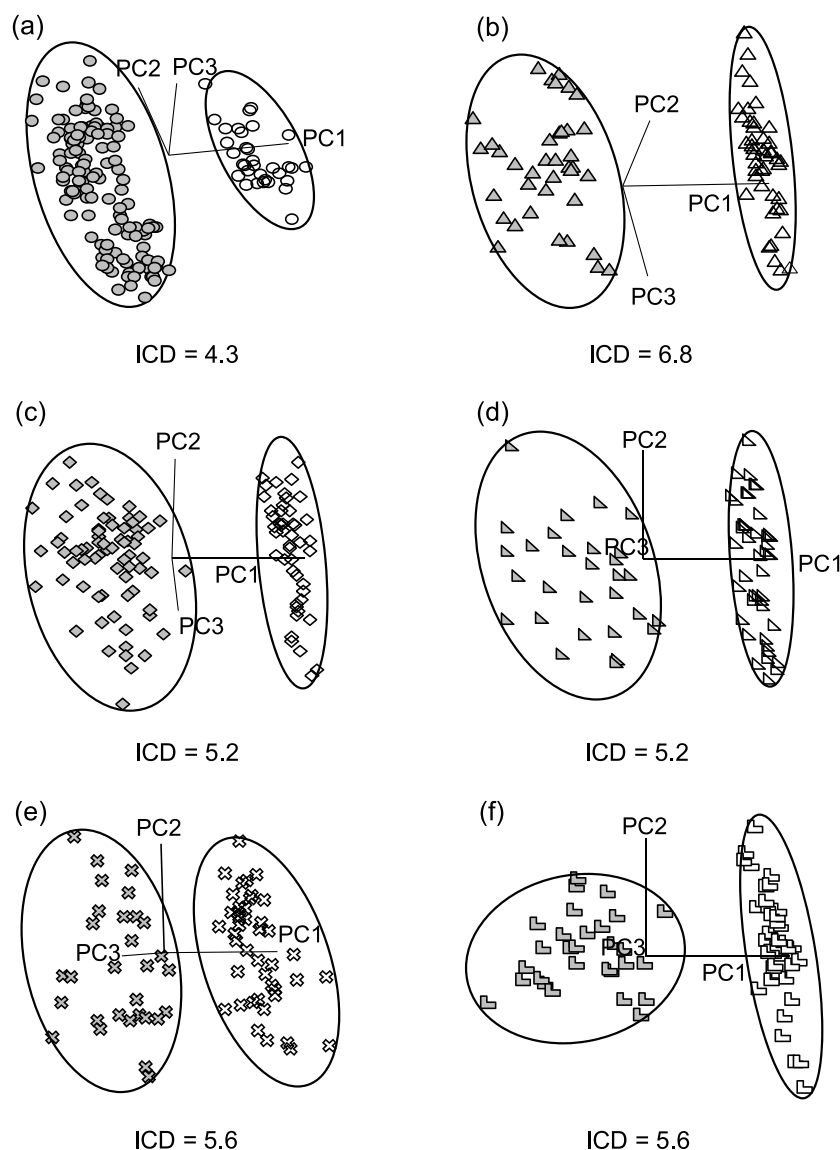


Fig. 3. SIMCA class projections plots and interclass distance (ICD) values of transformed (MSC and second derivative, 7 points width) diffuse reflectance near-infrared spectra of (a) N-S (○), (b) AD-S (△), (c) M-S (◇), (d) AD-SP (▽), (e) A/M-SP (⊗) and (f) M-SP (◻) cork stoppers. Untreated and treated stoppers are represented by blank and grey filled symbols, respectively.

distance. ICD values close to zero mean no differentiation while values greater than one indicate class separation (Wold & Sjöström, 1977). In general, two clusters of samples are considered significantly different when an ICD value above 3.0 is reached (Dunn & Wold, 1995). ICDs among cork stopper samples are displayed in Fig. 3 together with the class projections plots. ICD values greater than 3.0 (ranging from 4.3–6.8) were achieved for all compared cork stoppers, suggesting significant differences between treated and untreated cork samples for every type of closure.

In addition to providing class separation, residuals give valuable information of the strength of any given variable to discriminate among classes (Wold & Sjöström, 1977). The so-called discriminating power plots gather the spectral bands being responsible of the samples' differentiation. Discriminating power plots of all 2-class SIMCA models built up with NIR data are shown in Fig. 4. For all models except that of the natural cork stopper, same NIR bands were obtained related to the chemical composition of the surface treatments applied. The NIR bands located at 1933 and 2285–92 nm could be assigned to Si–O–H and Si–O–Si combination band (Si–O–H stretching + Si–O–Si deformation) and CH vibrations (second overtone bending) of silicone,

respectively (Workman & Weyer, 2008). Other NIR bands were also obtained at 2337 and 2367 nm, and may be attributed to CH combination band (C–H stretching + C–H deformation) of cellulose or silicone (Cai, Neyer, Kuckuk, & Heise, 2010; Schwanninger et al., 2011). Minor NIR bands also found in 1650–1800 nm region could be linked to CH groups (first overtone C–H stretching) of cellulose and lignin or silicone (Cai et al., 2010). Concerning natural cork stoppers, which were treated with a mixture of paraffin and silicone coating agents, other NIR bands were observed. The band at 2130 nm could be associated to CH and CO combination band (C–H stretching + C=O stretching) of cellulose (Schwanninger et al., 2011), while the bands located in the region between 2200–2400 nm might be related to CH₂ groups of paraffin (Workman & Weyer, 2008). All the chemical groups already discussed were also displayed in paraffin and silicone-treated cork stoppers through mid-infrared (MIR) spectroscopy in previous conducted studies (Gonzalez-Adrados et al., 2012; González-Gaitano & Ferrer, 2013; Ortega-Fernández, González-Adrados, García-Vallejo, Calvo-Haro, & Cáceres-Esteban, 2006), supporting the suitability of NIR spectroscopy coupled to pattern recognition techniques for monitoring the surface treatment of cork closures.

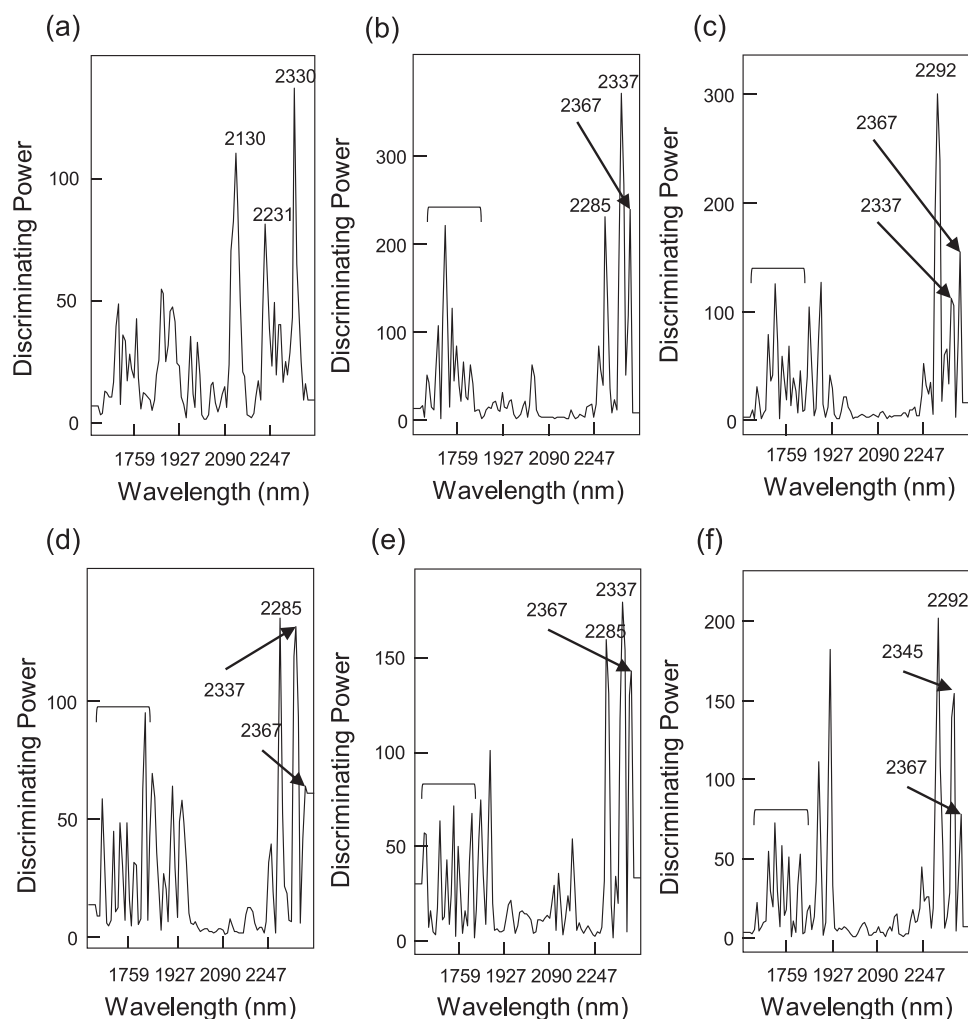


Fig. 4. SIMCA discriminating power plots of transformed (MSC and second derivative, 7 points width) diffusive reflectance near-infrared spectra of (a) N-S, (b) AD-S, (c) M-S, (d) AD-SP, (e) A/M-SP and (f) M-SP cork stoppers.

Besides the characterization of surface treatments, another SIMCA model including only untreated samples confirmed that there were no chemical differences between technical and agglomerated corks (Fig. S4 and Tables S3 and S4). Then, they were considered as a single class in a new model in order to assess its performance when obviating cork stopper's type (natural cork stoppers were excluded from the training set). Class projections and discriminating power plots of this model (Fig. 5a) proved that surface treatment can be authenticated through NIR analysis without taking into account closure's variety (except for natural cork stoppers), showing same separation and same NIR bands that in previous models (Fig. 4b–f), the latter being attributed to the main chemical groups of the surface coating agent applied (silicone).

Lastly, the classification performance of this model was tested using an external validation set. The model showed high specificity and sensitivity values, being 97.73 % (43/44 spectra) and 96.67 % (58/60 spectra) for the treated samples (5 samples analyzed, one for each variety except for the natural cork stoppers), respectively. Regarding untreated samples (5 samples analyzed, one for each variety except for the natural cork stoppers), the sensitivity and specificity were 93.33 % (56/60 spectra) and 100.00 % (44/44 spectra), respectively. Our results confirmed that the model developed is able to discriminate the treated corks from those without treatment.

3.4. Surface treatment authentication by Raman spectroscopy combined with SIMCA

The feasibility of Raman spectroscopy in surface treatment authentication was also studied in M-S P stoppers. Fig. 5b shows the class projections (with ICD value) and discriminating power plots obtained through SIMCA's algorithm. Tight clustering and clear differentiation were achieved with an ICD value of 3.7, confirming that treated and untreated M-S P stoppers were statistically different. Raman bands displayed in discriminating power plots were related to chemical components of silicone, such as 1477 and 1580 cm^{-1} (aromatic C–H bending and ring stretching of phenyl groups, respectively). The Raman bands around 477 – 509 cm^{-1} could be linked to Si–O–Si stretching of silicone, functional group also found in SIMCA models built up with NIR spectra (Cai et al., 2010). Raman spectroscopy provided complementary information about the treatments applied to cork stoppers, fitting with the data obtained through NIR spectroscopy.

3.5. Development of a PLSR calibration model for predicting extraction forces in cork stoppers using NIR data

A factor-based regression technique was selected instead of Multiple Linear Regression (MLR) due to the highly correlated nature of spectroscopic measurements. In PLSR, new uncorrelated variables are first obtained by establishing linear combinations of the original ones. Then, a regression model is performed following the least squares criterion (i.

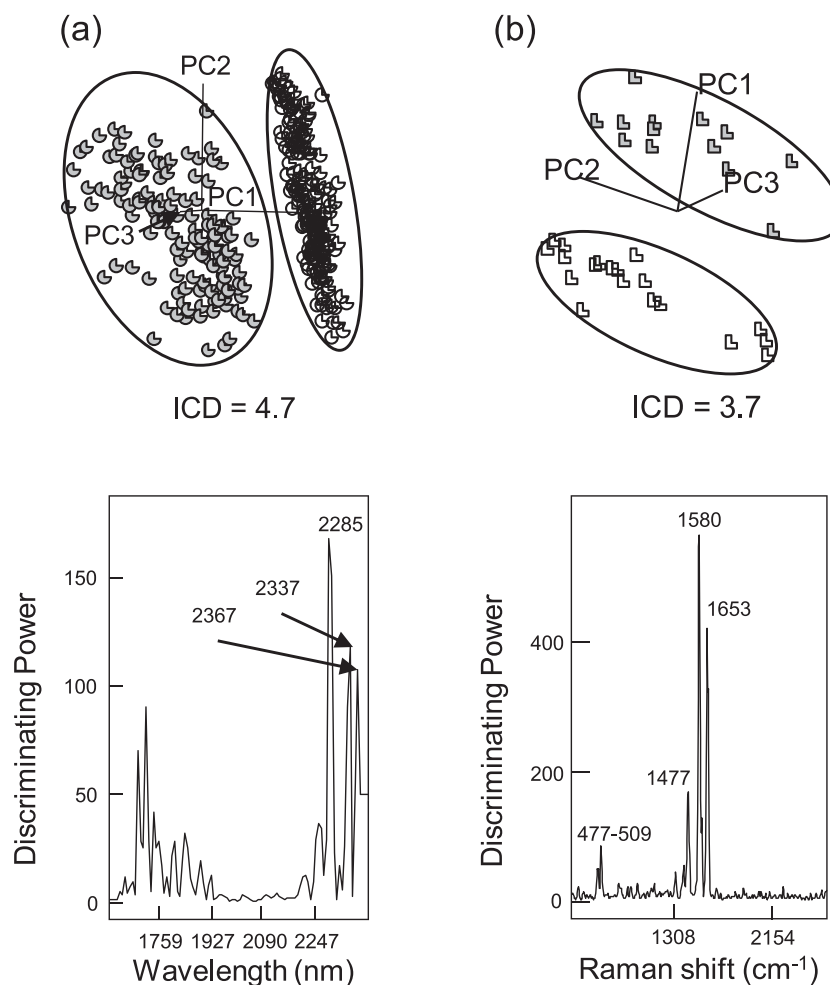


Fig. 5. SIMCA class projections and discriminating power plots of (a) transformed (MSC and second derivative, 7 points width) diffusive reflectance near-infrared spectra of all but not natural cork stoppers and (b) transformed (denoised and MSC corrected) transmission Raman spectra of M-SP cork stoppers. Untreated and treated stoppers are represented with blank and grey filled symbols, respectively. Interclass distance (ICD) values for (b) and (c) are also depicted.

e. minimizing the error sum of squares) (Martens & Næs, 1989).

Good linear correlations were observed between measured and predicted extraction force values in the 5-factor PLSR model built up (Table 2), with a coefficient of determination in validation (R^2_{VAL}) of 0.97 (Fig. S3). Moreover, the SECV and SEP values (i.e. estimators of the expected error of predicting the dependent variable of an unknown sample (Westad, Bevilacqua, & Marini, 2013)) were low (3.8 daN and 4.0 daN, respectively). The fact that SECV and SEP were comparable indicated that the calibration model can predict accurately the extraction force from new NIR data (i.e. external validation set) (Santos, Pereira-Filho, & Rodriguez-Saona, 2013). The model displayed a better predictive performance than those described in previous literature (Prades et al., 2014).

Additionally, the regression vector reveals which NIR bands are important in modelling the extraction force measurements (Martens & Næs, 1989). As expected, the NIR bands observed in the regression vector (represented in Fig. 6) were the same as those obtained in SIMCA's discriminating power plots, and were attributed to silicone (1691, 1716, 1742, 1919–43 and 2285 nm), polyurethane binder (2130 nm; adhesive used to bind the particles in agglomerated corks) and paraffin (around 2230 nm) (Cai et al., 2010; Miller & Eichinger, 1990; Schwanninger et al., 2011; Workman & Weyer, 2008). Our results suggest that the PLSR model built up can predict in a precise way the extraction force measurements based on the coating agents applied and the binder used to produce cork agglomerates.

Table 2

Extraction forces measured (reference method) and predicted using NIR data and partial least squares regression models.

Class	N-S		AD-S		M-S	
	Untreated	Treated	Untreated	Treated	Untreated	Treated
Measured	71.5 ± 17.9 ^a	22.3 ± 2.6	40.0 ± 3.8	24.4 ± 1.8	32.5 ± 1.7	30.8 ± 3.6
Pred _{CAL}	70.4 ± 4.0	22.4 ± 3.2	43.0 ± 2.9	24.3 ± 3.0	32.8 ± 2.8	30.2 ± 2.9
Pred _{VAL}	70.3 ± 4.2	22.4 ± 3.4	43.1 ± 3.1	24.3 ± 3.2	32.8 ± 2.9	30.2 ± 2.9
Predicted	69.1 ± 3.2	19.8 ± 3.9	41.8 ± 5.1	23.9 ± 4.3	32.7 ± 3.0	29.3 ± 5.1

^a Values are displayed as mean ± standard deviation. Abbreviations used: N-S, natural cork-still wine; AD-S, agglomerated cork with discs-still wine; M-S, micro-agglomerated cork-still wine; pred_{CAL}, predicted values based on the calibration step; pred_{VAL}, predicted values based on the cross-validation step; predicted, predicted values based on the external validation step.

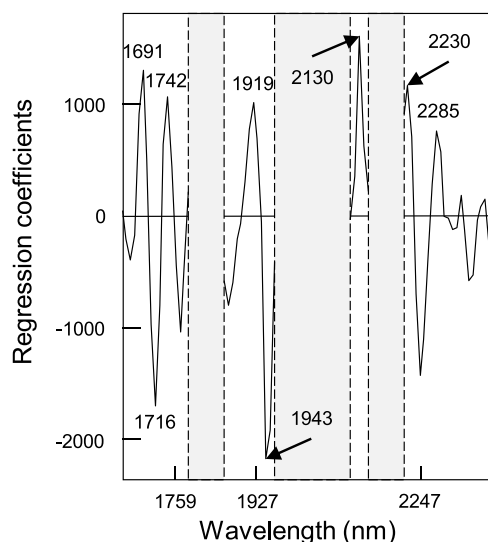


Fig. 6. PLSR regression vector obtained of transformed (MSC and second derivative, 7 points width) diffuse reflectance near-infrared spectra of treated and untreated still-wine cork stoppers (N-S, AD-S and M-S samples). Spectral regions discarded when building up the models are displayed in grey.

4. Conclusions

The evidence from the present work suggests that NIR spectroscopy combined with SIMCA provides a sensitive, rapid and easy tool for the quality assurance of the surface treatments applied to cork stoppers. Significant chemical differences were detected between surface treated and untreated cork stoppers, which were linked to several functional groups belonging to paraffin and silicone coating agents. In this regard, it was found that a lack of homogeneity of the surface treatments applied could be assumed due to the presence of outliers detected in treated corks that were classified as untreated ones. A 2-class SIMCA model was also developed including all cork stoppers treated in one class and those untreated in another, regardless of their variety. High classification rates for treated (97.73 %) and untreated samples (93.33 %) were displayed applying this model. Raman analysis was also conducted, and similar outcomes were obtained, confirming the band assignments attributed using NIR spectroscopy. Finally, PLSR models built up with NIR data showed good correlation with extraction force measurements performed, which were modelled through NIR bands linked to the coating agents applied and the binder used to produce the cork agglomerates. We believe that our findings will be valuable in solving the difficulty of assuring the presence and homogeneity of surface treatments applied to stoppers in a rapid way. This technique could also be implemented on-line, leading to a reduction of time and economic losses from the manufacturing perspective.

Funding

J. Mellado-Carretero is supported by a Martí Franquès scholarship (2018-PIPF-7).

CRediT authorship contribution statement

Jorge Mellado-Carretero: Investigation, Writing - original draft, Software, Formal analysis. **Didem Peren Aykas:** Investigation. **Miquel Puxeu:** Resources, Investigation. **Sylvana Varela:** Software, Formal analysis, Writing - review & editing. **Luis Rodriguez-Saona:** Resources, Writing - review & editing. **Diego García-Gonzalo:** Writing - review & editing. **Sílvia de Lamo-Castellví:** Conceptualization, Methodology, Supervision, Writing - review & editing.

Declaration of Competing Interest

None.

Acknowledgements

Thanks are due to S. Suñé (De Maria Taps S. L.), who gave us much valuable advice during all the stages of the work. J. Mellado-Carretero acknowledges N. García-Gutiérrez (Universitat Rovira i Virgili) for providing support when making the artwork.

Appendix A. Supplementary data

Supplementary material related to this article can be found, in the online version, at doi:<https://doi.org/10.1016/j.fpsl.2021.100680>.

References

- Asociación Española de Normalización y Certificación. (2001). *Three parts stoppers. Test methods and specifications* (UNE 56926) <https://www.une.org/encuentra-tu-norma/busca-tu-norma/norma?c=N0024786>.
- Asociación Española de Normalización y Certificación. (2003). *Natural cork stoppers for still wines. Test methods and specifications* (UNE 56921) <https://www.une.org/encuentra-tu-norma/busca-tu-norma/norma?c=N0064388>.
- Asociación Española de Normalización y Certificación. (2006). *Agglomerated cork stoppers with natural cork discs for sparkling wines. Test methods and specifications* (UNE 56923) <https://www.une.org/encuentra-tu-norma/busca-tu-norma/norma?c=N0036203>.
- Asociación Española de Normalización y Certificación. (2019). *Agglomerated microgranulated cork stoppers for still wines* (UNE 56933) <https://www.une.org/encuentra-tu-norma/busca-tu-norma/norma?c=N0061304>.
- Bevilacqua, M., Bucci, R., Magrì, A. D., Magrì, A. L., Nescatelli, R., & Marini, F. (2013). *Classification and class-modelling*. In F. Marini (Ed.), *Chemometrics in food chemistry* (pp. 171–192). Elsevier B.V.
- Cai, D., Neyer, A., Kuckuk, R., & Heise, H. M. (2010). Raman, mid-infrared, near-infrared and ultraviolet-visible spectroscopy of PDMS silicone rubber for characterization of polymer optical waveguide materials. *Journal of Molecular Structure*, 976, 274–281. <https://doi.org/10.1016/j.molstruc.2010.03.054>
- Dunn, W. J., & Wold, S. (1995). SIMCA pattern recognition and classification. In H. van de Waterbeemd (Ed.), *Chemometric methods in molecular design* (pp. 179–192). VCH Publishers, Inc.
- Fernández Pierna, J. A., Manley, M., Dardenne, P., Downey, G., & Baeten, V. (2018). *Spectroscopic technique: Fourier Transform (FT) Near-Infrared Spectroscopy (NIR) and Microscopy (NIRM)*. In D.-W. Sun (Ed.), *Modern techniques for food authentication* (pp. 103–138). Elsevier, Inc.
- Fugelsang, K. C., Callaway, D., Toland, T., & Muller, C. J. (1997). *Coating agents for corks*. *Wine Industry Journal*, 12, 185–187.
- Gierlinger, N., & Schwanninger, M. (2006). Chemical imaging of poplar wood cell walls by confocal Raman microscopy. *Plant Physiology*, 140, 1246–1254. <https://doi.org/10.1104/pp.105.066993.1246>
- Giunchi, A., Versari, A., Parpinello, G. P., & Galassi, S. (2008). Analysis of mechanical properties of cork stoppers and synthetic closures used for wine bottling. *Journal of Food Engineering*, 88, 576–580. <https://doi.org/10.1016/j.jfoodeng.2008.03.004>
- González-Adrados, J. R., García-Vallejo, M. C., Cáceres-Esteban, M. J., García de Ceca, J. L., González-Hernández, F., & Calvo-Haro, R. (2012). Control by ATR-FTIR of surface treatment of cork stoppers and its effect on their mechanical performance. *Wood Science and Technology*, 46, 349–360. <https://doi.org/10.1007/s00226-011-0403-5>
- González-Gaitano, G., & Ferrer, M. A. C. (2013). Definition of QC parameters for the practical Use of FTIR-ATR spectroscopy in the analysis of surface treatment of cork stoppers. *Journal of Wood Chemistry and Technology*, 33, 217–233. <https://doi.org/10.1080/02773813.2013.779715>
- Jackson, R. S. (2014). Post-fermentation treatments and related topics. In R. S. Jackson (Ed.), *Wine science* (pp. 535–676). Elsevier Inc.
- Jung, R., & Schaefer, V. (2010). Reducing cork taint in wine. In A. G. Reynolds (Ed.), *Managing wine quality* (pp. 388–417). Woodhead Publishing Limited.
- Kvalheim, O. M., & Karstang, T. V. (1992). SIMCA - Classification by means of disjoint cross validated principal components models. In R. G. Brereton (Ed.), *Multivariate pattern recognition in chemometrics: Illustrated by case studies* (pp. 209–248). Elsevier Science Publishers B.V.
- Martens, H., & Næs, T. (1989). *Multivariate calibration*. John Wiley & Sons, Inc.
- McClure, W. F. (2006). Introduction. In Y. Ozaki, W. F. McClure, & A. A. Christy (Eds.), *Near-infrared spectroscopy in food science and technology* (pp. 1–10). John Wiley and Sons, Inc.
- Miller, C. E., & Eichinger, B. E. (1990). Analysis of rigid polyurethane foams by near-infrared diffuse reflectance spectroscopy. *Applied Spectroscopy*, 44, 887–894. <https://doi.org/10.1366/0003702904087064>
- Ortega-Fernández, C., González-Adrados, J. R., García-Vallejo, M. C., Calvo-Haro, R., & Cáceres-Esteban, M. J. (2006). Characterization of surface treatments of cork stoppers by FTIR-ATR. *Journal of Agricultural and Food Chemistry*, 54, 4932–4936. <https://doi.org/10.1021/jf0529823>

- Osten, D. W. (1988). Selection of optimal regression models via cross-validation. *Journal of Chemometrics*, 2, 39–48. <https://doi.org/10.1002/cem.1180020106>
- Pereira, H. (2007a). Production of cork stoppers and discs. In H. Pereira (Ed.), *Cork: Biology, production and uses* (pp. 263–288). Elsevier B.V.
- Pereira, H. (2007b). Wine and cork. In H. Pereira (Ed.), *Cork: Biology, production and uses* (pp. 305–327). Elsevier B.V.
- Porep, J. U., Kammerer, D. R., & Carle, R. (2015). On-line application of near infrared (NIR) spectroscopy in food production. *Trends in Food Science & Technology*, 46, 211–230. <https://doi.org/10.1016/j.tifs.2015.10.002>
- Prades, C., García-Olmo, J., Romero-Prieto, T., García de Ceca, J. L., & López-Luque, R. (2010). Methodology for cork plank characterization (*Quercus suber* L.) by near-infrared spectroscopy and image analysis. *Measurement Science & Technology*, 21, 065602. <https://doi.org/10.1088/0957-0233/21/6/065602>
- Prades, C., Gómez-Sánchez, I., García-Olmo, J., & González-Adrados, J. R. (2012). Discriminant analysis of geographical origin of cork planks and stoppers by near infrared spectroscopy. *Journal of Wood Chemistry and Technology*, 32, 66–85. <https://doi.org/10.1080/02773813.2011.599697>
- Prades, C., Gómez-Sánchez, I., García-Olmo, J., González-Hernández, F., & González-Adrados, J. R. (2014). Application of VIS/NIR spectroscopy for estimating chemical, physical and mechanical properties of cork stoppers. *Wood Science and Technology*, 48, 811–830. <https://doi.org/10.1007/s00226-014-0642-3>
- Sánchez-González, M., & Pérez-Terrazas, D. (2018). Assessing the percentage of cork that a stopper should have from a mechanical perspective. *Food Packaging and Shelf Life*, 18, 212–220. <https://doi.org/10.1016/j.fpsl.2018.10.009>
- Sánchez-González, M., García-Olmo, J., & Prades, C. (2016). Correlation between porosity of cork planks before and after boiling using near infrared spectroscopy. *European Journal of Wood and Wood Products*, 74, 509–517. <https://doi.org/10.1007/s00107-016-1014-5>
- Santos, P. M., Pereira-Filho, E. R., & Rodriguez-Saona, L. E. (2013). Application of hand-held and portable infrared spectrometers in bovine milk analysis. *Journal of Agricultural and Food Chemistry*, 61, 1205–1211. <https://doi.org/10.1021/jf303814g>
- Schwanninger, M., Rodrigues, J. C., & Fackler, K. (2011). A Review of band assignments in near infrared spectra of wood and wood components. *Journal of Near Infrared Spectroscopy*, 19, 287–308. <https://doi.org/10.1255/jnirs.955>
- Shah, N. K., & Gemperline, P. J. (1990). Combination of the mahalanobis distance and residual variance pattern recognition techniques for classification of near-infrared reflectance spectra. *Analytical Chemistry*, 62, 465–470. <https://doi.org/10.1021/ac00204a009>
- Silva, S. P., Sabino, M. A., Fernandes, E. M., Correlo, V. M., Boesel, L. F., & Reis, R. L. (2008). Cork: Properties, capabilities and applications. *International Materials Reviews*, 53, 256. <https://doi.org/10.1179/174328008X353529>
- Tshabalala, M. A., Jakes, J., VanLandingham, M. R., Wang, S., & Peltonen, J. (2012). Surface characterization. In R. M. Rowell (Ed.), *Handbook of wood chemistry and wood composites*. Taylor & Francis Group, LLC.
- Weisberg, S. (2005). Weights, lack of fit, and more. *Applied linear regression* (pp. 96–114). John Wiley & Sons, Inc..
- Westad, F., Bevilacqua, M., & Marini, F. (2013). Regression. In F. Marini (Ed.), *Chemometrics in food chemistry* (pp. 127–170). Elsevier B.V.
- Wold, S. (1976). Pattern recognition by means of disjoint principal components models. *Pattern Recognition*, 8, 127–139. [https://doi.org/10.1016/0031-3203\(76\)90014-5](https://doi.org/10.1016/0031-3203(76)90014-5)
- Wold, S., & Sjöström, M. (1977). SIMCA: A method for analyzing chemical data in terms of similarity and analogy. In B. R. Kowalski (Ed.), *Chemometrics: Theory and application* (pp. 243–282). ACS Publications.
- Workman, J., & Weyer, L. (2008). Spectra-structure correlations: Labeled spectra from 7200 cm⁻¹ to 3800 cm⁻¹ (1389 nm to 2632 nm). *Practical guide to interpretive near-infrared spectroscopy*, 165–206.